



The atomic-scale finite element method

B. Liu, Y. Huang^{a,*}, H. Jiang^a, S. Qu^a, K.C. Hwang^b

^a *Department of Mechanical and Industrial Engineering, University of Illinois at Urbana-Champaign, 1206 West Green Street, Urbana, IL 61801, USA*

^b *Department of Engineering Mechanics, Tsinghua University, Beijing 100084, China*

Received 2 June 2003; received in revised form 13 October 2003; accepted 2 December 2003

Abstract

The multiscale simulation is important to the development of nanotechnology and to the study of materials and systems across multiple length scales. In order to develop an efficient and accurate multiscale computation method within a unified theoretical framework, we propose an order- N atomic-scale finite element method (AFEM). It is as accurate as molecular mechanics simulations, but is much faster than the widely used order- N^2 conjugate gradient method. The combination of AFEM and continuum finite element method provides a seamless multiscale computation method suitable for large scale static problems.

© 2004 Elsevier B.V. All rights reserved.

Keywords: Atomic scale; Finite element method; Order- N ; Multiscale computation

1. Introduction

The fastest supercomputer in the world can handle up to a billion atoms today in molecular dynamics simulations [3,4], which correspond only to a small cube of 1 μm in size. Even with the rapid advance in computer power, this size may increase to only 10 μm in 15 years since the computer power doubles every 18 months (Moore's law [18]). This size limit of computation is far short to reach the macroscale such that molecular dynamics alone cannot predict the properties and response of macroscopic materials directly from their nano- and micro-structures. Other atomistic methods also have difficulties for large systems. For example, the widely used conjugate gradient method in molecular mechanics is an order- N^2 method whose computational effort increases with the square of system size N . It is therefore not suitable for large systems, nor for the rapid simulation of nanoscale components that are up to a few hundred nanometers in size.

On the other hand, the conventional continuum methods such as the finite element method (FEM) are not applicable to nanoscale components because they are developed for macroscale problems. The macroscale material behaviors are incorporated in the conventional continuum FEM via the constitutive

* Corresponding author. Tel.: +1-217-2655072; fax: +1-217-2446534.
E-mail address: huang9@uiuc.edu (Y. Huang).

models of solids, which are usually empirical and are determined from macroscale experiments such as simple tension tests. These constitutive models represent the collective behavior of many atoms, and cannot accurately predict the response of discrete atoms. For example, for a uniform deformation on the macroscale (as in a simple tension test), the atomic motion may not be uniform at the atomic scale even for a perfect atomic structure without defects [30,31]. Furthermore, most atomistic interactions are multi-body in nature, i.e., the energy in an atomic bond between a pair of atoms depends on the positions of atoms both in and outside the pair (e.g., [6,7]). This “non-local” dependence of energy is inconsistent with the macroscopic, local constitutive model in the conventional FEM.

Since the atomistic simulations and continuum FEM have difficulties to “scale up” and “scale down”, respectively, multiscale computation methods have emerged as a viable means to study materials and systems across different length scales (e.g., [2,8–10,16,20,21,26,28]). The basic idea is to combine the atomistic simulation methods which capture the nanoscale physics laws with the continuum FEM which represents the collective behavior of atoms but significantly reduces the degrees of freedom. One approach is to use the atomistic simulation methods for domains in which the discrete motion of atoms is important and must be accounted for, and use the continuum FEM for the rest where the response of materials and systems can be represented by the continuum models [9,10,16,20,21,28]. Such an approach involves artificially introduced interfaces between domains of atomistic and continuum simulation methods. It requires the interface conditions, which add significant computational efforts, and may lead to computation errors. Another approach in the atomistic–continuum linkage is quasicontinuum method [22–24]. The interatomic potential is directly incorporated into the continuum FEM method via the Cauchy–Born rule (e.g., [5]) to obtain the continuum strain energy density from the energy stored in atomic bonds. The quasicontinuum method involves both discrete atoms and continuum solids, and the method can also account for the non-local effect [22,24], i.e., the multi-body atomistic interactions. However, the spurious or “ghost” force appears at the interface between the domains of (local) continuum and (non-local) atomistic simulations in the quasicontinuum method [22]. The quasicontinuum analysis uses the conjugate gradient method [23], which is an order- N^2 method and is not suitable for large problems. Recently, Wagner and Liu [26] coupled the atomistic and continuum simulations using a bridging scale decomposition.

In this paper we develop an order N , atomic-scale finite element method (AFEM) that is as accurate as molecular mechanics simulations. It can be linked seamlessly with the continuum FEM since they are within the same theoretical framework (of FEM). The AFEM can handle discrete atoms and account for the multi-body interactions among atoms. It is an order- N method (i.e., the computation scales linearly with the system size), and is therefore much faster than the (order- N^2) conjugate gradient method widely used in atomistic studies. The vast increase in speed of AFEM makes it possible to study large scale problems that would take unbearable amount of time with the existing methods. Furthermore, the seamless linkage between AFEM and FEM provides a powerful multiscale computation method that significantly reduces the degree of freedom and enables the computation for a much larger scale (possibly macroscale) static systems.

The paper is structured in the following way. We present the AFEM elements for a one-dimensional atomic chain and for carbon nanotubes in Section 2. The order- N nature and the stability of AFEM are discussed in Sections 3 and 4, respectively. Section 5 presents the AFEM/FEM multiscale computation method. A transitional element between AFEM and continuum FEM elements is also developed. The AFEM is used to study a carbon nanotube knot, and the vibration of a carbon nanotube in Section 7.

2. Atomic-scale finite elements

The equilibrium configuration of solids corresponds to a state of minimal energy. The basic idea of conventional continuum finite element method is to divide a continuum solid into finite number of ele-

ments, and each element is characterized by a finite set of discrete nodes. The positions of all nodes are determined by minimizing the energy in the solid. This is similar to the molecular mechanics calculations of atom positions, which is based on the energy minimization with respect to discrete atoms. Therefore, the continuum FEM and molecular mechanics share a common ground of energy minimization, with respect to the nodes and to the discrete atoms, respectively.

For a system of N atoms, the energy stored in the atomic bonds is denoted by $U_{\text{tot}}(\mathbf{x}_1, \mathbf{x}_2, \dots, \mathbf{x}_N)$, where \mathbf{x}_i is the position of atom i . An example of U_{tot} is

$$U_{\text{tot}} = \sum_{i < j}^N U(\mathbf{x}_j - \mathbf{x}_i) \tag{1}$$

for atoms characterized by a pair interatomic potential U such as the Lennard-Jones potential. For a multi-body interatomic potential (e.g., [6,7]), the energy U in an atomic bond also depends on atoms outside the bond.

The total energy is

$$E_{\text{tot}}(\mathbf{x}) = U_{\text{tot}}(\mathbf{x}) - \sum_{i=1}^N \bar{\mathbf{F}}_i \cdot \mathbf{x}_i, \tag{2}$$

where $\mathbf{x} = (\mathbf{x}_1, \mathbf{x}_2, \dots, \mathbf{x}_N)^T$, and $\bar{\mathbf{F}}_i$ is the external force (if there is any) exerted on atom i . The state of minimal energy corresponds to

$$\frac{\partial E_{\text{tot}}}{\partial \mathbf{x}} = 0. \tag{3}$$

The Taylor expansion of E_{tot} around an initial guess $\mathbf{x}^{(0)} = (\mathbf{x}_1^{(0)}, \mathbf{x}_2^{(0)}, \dots, \mathbf{x}_N^{(0)})^T$ of the equilibrium state gives

$$E_{\text{tot}}(\mathbf{x}) \approx E_{\text{tot}}(\mathbf{x}^{(0)}) + \left. \frac{\partial E_{\text{tot}}}{\partial \mathbf{x}} \right|_{\mathbf{x}=\mathbf{x}^{(0)}} \cdot (\mathbf{x} - \mathbf{x}^{(0)}) + \frac{1}{2} (\mathbf{x} - \mathbf{x}^{(0)})^T \cdot \left. \frac{\partial^2 E_{\text{tot}}}{\partial \mathbf{x} \partial \mathbf{x}} \right|_{\mathbf{x}=\mathbf{x}^{(0)}} \cdot (\mathbf{x} - \mathbf{x}^{(0)}). \tag{4}$$

Its substitution into Eq. (3) yields the following governing equation for the displacement $\mathbf{u} = \mathbf{x} - \mathbf{x}^{(0)}$,

$$\mathbf{K}\mathbf{u} = \mathbf{P}, \tag{5}$$

where

$$\mathbf{K} = \left. \frac{\partial^2 E_{\text{tot}}}{\partial \mathbf{x} \partial \mathbf{x}} \right|_{\mathbf{x}=\mathbf{x}^{(0)}} = \left. \frac{\partial^2 U_{\text{tot}}}{\partial \mathbf{x} \partial \mathbf{x}} \right|_{\mathbf{x}=\mathbf{x}^{(0)}}$$

is the stiffness matrix,

$$\mathbf{P} = - \left. \frac{\partial E_{\text{tot}}}{\partial \mathbf{x}} \right|_{\mathbf{x}=\mathbf{x}^{(0)}} = \bar{\mathbf{F}} - \left. \frac{\partial U_{\text{tot}}}{\partial \mathbf{x}} \right|_{\mathbf{x}=\mathbf{x}^{(0)}}$$

is the non-equilibrium force vector, and $\bar{\mathbf{F}} = (\bar{\mathbf{F}}_1, \bar{\mathbf{F}}_2, \dots, \bar{\mathbf{F}}_N)^T$. Except for a linear system, Eq. (5) is solved iteratively until \mathbf{P} reaches zero, $\mathbf{P} = 0$. It is observed that the governing equation in FEM is identical to Eq. (5) if the FEM nodes are taken as atoms.

The stiffness matrix \mathbf{K} and non-equilibrium force vector \mathbf{P} are evaluated in each iteration step. In conventional continuum FEM, the total energy is partitioned into elements. The energy in each element is obtained in terms of only the nodes in the element. For atomistic interactions characterized by a pair potential (1), \mathbf{K} and \mathbf{P} can be obtained straightforwardly via the continuum conventional FEM since the

pair potential can be equivalently represented by a (nonlinear) string element. For multi-body interatomic potentials, however, the energy in an atomic bond between a pair of atoms is influenced by atoms outside the pair. A conventional FEM element cannot capture this non-local dependence of energy since it requires the information (e.g., atoms) beyond the element. This will be further illustrated in two examples for a one-dimensional atomic chain and a carbon nanotube in this section.

We will develop an AFEM in order to capture the multi-body atomistic interactions. Unlike conventional continuum FEM, we do not divide energy into elements but calculate the first and second order derivatives of E_{tot} needed in the governing equation, Eq. (5), directly from this single AFEM element.

2.1. AFEM element for one-dimensional chain of atoms

We consider a one-dimensional atomic chain of N atoms shown in Fig. 1a. For the atomic bond between atoms $i - 1$ and i ($3 \leq i \leq N - 1$), one example of the multi-body interatomic potential is

$$U_{(i-1,i)} = U(x_i - x_{i-1}; x_{i-1} - x_{i-2}) + U(x_i - x_{i-1}; x_{i+1} - x_i). \tag{6}$$

The two terms on the right hand side of the above equation reflect the interactions of this bond with the bonds on the left and right, respectively. A conventional FEM element between atoms $i - 1$ and i cannot evaluate the above energy (and its derivatives) since the element does not contain information about atoms $i - 2$ and $i + 1$ outside the bond.

Fig. 1b shows the AFEM element for atom i in this atomic chain. For the interatomic potential in (6), the first order derivative of U_{tot} with respect to atom i is

$$\frac{\partial U_{\text{tot}}}{\partial x_i} = \frac{\partial [U_{(i-2,i-1)} + U_{(i-1,i)} + U_{(i,i+1)} + U_{(i+1,i+2)}]}{\partial x_i}, \tag{7}$$

which depends on not only the nearest-neighbor atoms ($i - 1$ and $i + 1$) but also the second nearest-neighbor atoms ($i - 2$ and $i + 2$) of atom i . The non-zero components of the second order derivatives are $\frac{\partial^2 U_{\text{tot}}}{\partial x_i \partial x_j}$, $i - 2j + 2$. The AFEM element in Fig. 1b includes all neighbor atoms that interact with atom i .

It is noted that such an AFEM element overlaps in space with neighbor elements. In fact, this overlap enables us to accurately account for the non-local (multi-body) effect within a single element. As discussed in the following, such an overlap does not double count the element contribution to the global stiffness matrix \mathbf{K} and non-equilibrium force vector \mathbf{P} . The element stiffness matrix for atom i is given by

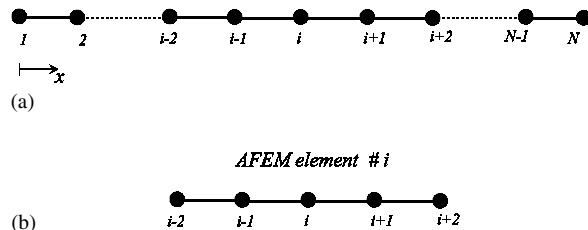


Fig. 1. (a) A schematic diagram of a one-dimensional atomic chain, (b) an atomic-scale finite element for the one-dimensional atomic chain accounting for multi-body atomistic interactions.

$$\mathbf{K}_i^{\text{element}} = \begin{bmatrix} \frac{\partial^2 U_{\text{tot}}}{\partial x_i \partial x_i} & \frac{1}{2} \frac{\partial^2 U_{\text{tot}}}{\partial x_{i-1} \partial x_i} & \frac{1}{2} \frac{\partial^2 U_{\text{tot}}}{\partial x_{i-2} \partial x_i} & \frac{1}{2} \frac{\partial^2 U_{\text{tot}}}{\partial x_{i+1} \partial x_i} & \frac{1}{2} \frac{\partial^2 U_{\text{tot}}}{\partial x_{i+2} \partial x_i} & \#i \\ \frac{1}{2} \frac{\partial^2 U_{\text{tot}}}{\partial x_{i-1} \partial x_i} & 0 & 0 & 0 & 0 & \#i - 1 \\ \frac{1}{2} \frac{\partial^2 U_{\text{tot}}}{\partial x_{i-2} \partial x_i} & 0 & 0 & 0 & 0 & \#i - 2 \\ \frac{1}{2} \frac{\partial^2 U_{\text{tot}}}{\partial x_{i+1} \partial x_i} & 0 & 0 & 0 & 0 & \#i + 1 \\ \frac{1}{2} \frac{\partial^2 U_{\text{tot}}}{\partial x_{i+2} \partial x_i} & 0 & 0 & 0 & 0 & \#i + 2 \end{bmatrix} \quad (8)$$

The element stiffness matrices associated with four atoms at or near the two ends, #1, 2, $N - 1$ and N , are either 3×3 or 4×4 . The non-equilibrium force vector for this element is

$$\mathbf{P}_i^{\text{element}} = \begin{bmatrix} \overline{F}_i - \frac{\partial U_{\text{tot}}}{\partial x_i} & \#i \\ 0 & \#i - 1 \\ 0 & \#i - 2 \\ 0 & \#i + 1 \\ 0 & \#i + 2 \end{bmatrix} \quad (9)$$

The above element stiffness matrix and non-equilibrium force vector are accurate because they do not involve any approximations of conventional FEM, such as the use of shape functions within the element, and the neglect of non-local effect in a local element. By the standard assembly in FEM, the global stiffness matrix \mathbf{K} and non-equilibrium force vector \mathbf{P} for the system are readily obtained from their counterparts at the element level. Contrary to conventional FEM, the i th row of the global stiffness matrix \mathbf{K} and the i th component of the non-equilibrium force vector \mathbf{P} are completely determined by this single AFEM element for atom i . Although the AFEM elements overlap in space, there is no double count of contributions to \mathbf{K} and \mathbf{P} from AFEM elements.

2.2. AFEM element for carbon nanotubes

It is important to note that the AFEM elements are material specific, i.e., they depend not only on the atomic structure but also on the atomistic interactions (e.g., nearest-neighbor and second nearest-neighbor interactions). We develop a three-dimensional AFEM element for carbon nanotubes in this section. Fig. 2a shows a single wall carbon nanotube consisting of a single layer of carbon atoms with the hexagonal lattice structure. Each carbon atom interacts with both nearest- and second nearest-neighbor atoms [6,7], and the latter results from the bond angle dependence in the interatomic potential. Since each carbon atom on a carbon nanotube has three nearest-neighbor atoms and six second nearest-neighbor atoms, the AFEM element consists of 10 carbon atoms as shown in Fig. 2b, namely the central atom #1, nearest-neighbor atoms #2, 5 and 8, and second nearest-neighbor atoms #3, 4, 6, 7, 9 and 10. Such an element captures the interactions between the central atom and other carbon atoms. The position change of the central atom 1 influences only the energy stored in nine atomic bonds in this AFEM element.

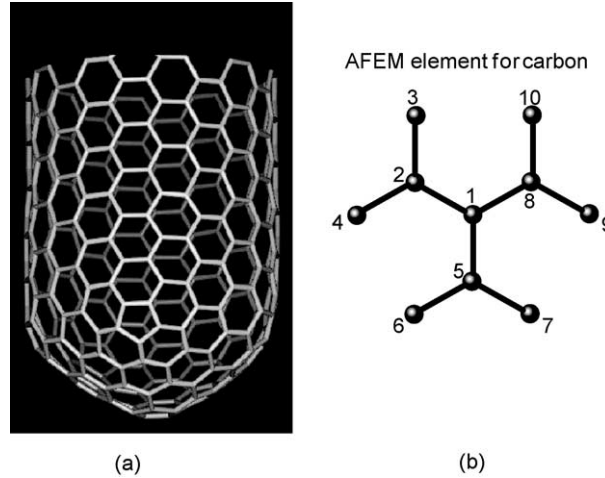


Fig. 2. (a) A schematic diagram of a single wall carbon nanotube, (b) an atomic-scale finite element for carbon nanotubes.

The element stiffness matrix and the non-equilibrium force vector are given by

$$\mathbf{K}^{\text{element}} = \begin{bmatrix} \left(\frac{\partial^2 U_{\text{tot}}}{\partial \mathbf{x}_1 \partial \mathbf{x}_1} \right)_{3 \times 3} & \left(\frac{1}{2} \frac{\partial^2 U_{\text{tot}}}{\partial \mathbf{x}_1 \partial \mathbf{x}_i} \right)_{3 \times 27} \\ \left(\frac{1}{2} \frac{\partial^2 U_{\text{tot}}}{\partial \mathbf{x}_i \partial \mathbf{x}_1} \right)_{27 \times 3} & (\mathbf{0})_{27 \times 27} \end{bmatrix}, \quad (10)$$

$$\mathbf{P}^{\text{element}} = \begin{bmatrix} \left(\bar{\mathbf{F}}_1 - \frac{\partial U_{\text{tot}}}{\partial \mathbf{x}_1} \right)_{3 \times 1} \\ (\mathbf{0})_{27 \times 1} \end{bmatrix}, \quad (11)$$

where i ranges from 2 to 10 in $\frac{\partial^2 U_{\text{tot}}}{\partial \mathbf{x}_1 \partial \mathbf{x}_i}$, and $\bar{\mathbf{F}}_1$ is the external force (if there is) exerted on the central atom in this element. It is observed that the non-zero components in the above element stiffness matrix are limited to the top three rows and left three columns. This is very different from the element stiffness matrix in conventional FEM because the AFEM element focuses on the “central” atom. The non-equilibrium force vector given in (11) shares the same feature, so do the $\mathbf{K}^{\text{element}}$ and $\mathbf{P}^{\text{element}}$ in Eqs. (8) and (9) for the one-dimensional atom chain.

Similar to conventional FEM, the global stiffness matrix \mathbf{K} for the system is sparse. This is because each row of \mathbf{K} is obtained from a single AFEM element. For carbon nanotubes, the AFEM element has (at most) 30 non-zero elements in each row (see Eq. (10)). Therefore, the number of non-zero components in \mathbf{K} is approximately $30 \times N$, which is on the order N , i.e., $O(N)$, where N is the total number of atoms in the system. It should be pointed out that the number of non-zero components in each row is governed by the non-local atomistic interactions. In the limit of local iterations, each atom interacts with three nearest-neighbor atoms such that the number of non-zero components becomes 12. Therefore, \mathbf{K} for non-local atomistic interactions is less sparse than that for local interactions, but it is still a sparse matrix with the number of non-zero components on the order of N . This observation holds for other material systems as long as each atom interacts with a finite number of atoms in the neighbor. For order- N sparse \mathbf{K} , the computational effort to solve $\mathbf{K}\mathbf{u} = \mathbf{P}$ in Eq. (5) is also on the order of N [19].

3. The order- N nature of AFEM

We show in this section that AFEM is an order- N method, while the widely used conjugate gradient method in molecular mechanics is an order- N^2 method. We first use a one-dimensional chain of atoms connected by linear springs. The last atom is fixed and the system is at equilibrium before a force is imposed on the first atom. The conjugate gradient method involves only the first order derivative of the energy, i.e., the non-equilibrium force P_i on atom i . Therefore, atom i will not move unless $P_i \neq 0$. Only the first atom (subject to the external force) moves during the first iteration searching for the minimal energy. Once the first atom moves, the second atom senses the non-equilibrium force and its motion is determined in the second iteration step. The motion of atoms gradually propagates to the rest of atoms, and it takes N steps to reach the last atom. Since the non-equilibrium force \mathbf{P} is evaluated for all N atoms within each iteration, the total computational effort for the conjugate gradient method is on the order of $O(N \times N) = O(N^2)$, i.e., an order- N^2 method. Other simulation methods based only on the first order derivative of energy, such as the steepest descent method and MD calculations of the equilibrium state, are also (at least) order- N^2 methods. If the springs in Fig. 3 are nonlinear, more computation efforts are needed such that these methods based on the first order derivative are (at least) order N^2 .

Because AFEM uses both first and second order derivatives of the energy, it takes one iteration step to reach the minimal energy for the linear one-dimensional atomic chain as well as for general linear systems. The computational effort of AFEM within each iteration step is composed of two parts:

- (i) the computation of the stiffness matrix \mathbf{K} and non-equilibrium force vector \mathbf{P} , which is on the order N since the number of non-zero components of \mathbf{K} and \mathbf{P} is proportional to N ;
- (ii) the effort to solve $\mathbf{K}\mathbf{u} = \mathbf{P}$ in Eq. (5), which is also on the order N due to the sparseness of \mathbf{K} [19].

Therefore, the computational effort for a general linear system is on the order of N . For a nonlinear system, Eq. (5) has to be solved iteratively, and the computational effort is on the order of $O(N \times M)$, where M is the number of iteration steps to reach minimal energy. As shown in the following example, M is essentially independent of N such that the computational effort is still on the order $O(N)$.

Fig. 4 shows the number of iteration steps M and deformed configurations for four (5,5) armchair carbon nanotubes with 400, 800, 1600 and 3200 atoms. The carbon nanotubes, which are initially straight with two ends fixed, are subject to the same lateral force $50 \text{ eV/nm} = 8.0 \text{ nN}$ in the middle. The number of iteration steps M varies very little with N (number of atoms), from 43 to 31 and averaged at 35. In fact, the CPU time (on a personal computer with 2.8 GHz CPU and 1 GB memory) shown in Fig. 4 indeed displays an approximate linear dependence on N . We have also calculated a much longer (5,5) carbon nanotube with 48,200 atoms, which has the same length of 605 nm as in Tomblor et al.'s experiments [25]. The number of iteration steps is 35, which is in the same range as those in Fig. 4. This example demonstrates that AFEM is essentially an order- N method and is therefore suitable for large scale computation.

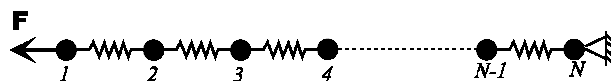


Fig. 3. A schematic diagram of a one-dimensional atomic chain connected by linear springs. The two ends are subject to a force and a vanishing displacement, respectively.

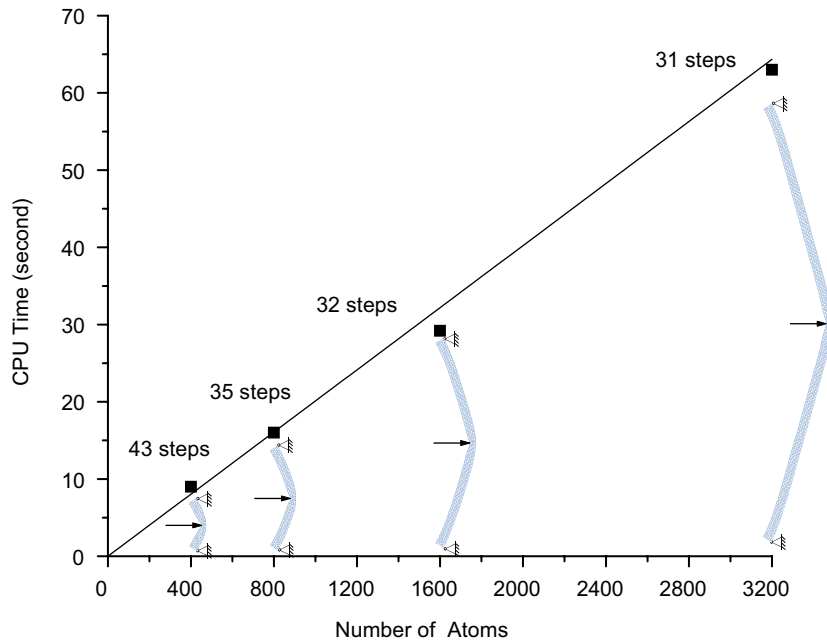


Fig. 4. The CPU time for AFEM scales linearly with number of atoms for (5,5) carbon nanotubes. The numbers of iteration steps is approximately independent of the atom number, which implies that AFEM is an order- N method.

4. Stability of AFEM

In this section, we study the stability and convergence of AFEM for nonlinear interatomic potentials that may display softening behavior. This instability may occur due to geometric or material nonlinearities. The stability and convergence are ensured if the energy in the system decreases in every step, i.e., $\mathbf{u} \cdot \mathbf{P} > 0$, where \mathbf{u} is the displacement increment, and \mathbf{P} is the non-equilibrium force in Eq. (5) and it represents the steepest descent direction of E_{tot} . From Eq. (5), a sufficient condition for $\mathbf{u} \cdot \mathbf{P} > 0$ is that the stiffness matrix \mathbf{K} is positive definite. For problems involving neither material softening nor nonlinear bifurcation, \mathbf{K} is usually positive definite and AFEM is stable, as in the examples in Fig. 4. For non-positive definite \mathbf{K} , we replace \mathbf{K} by $\mathbf{K}^* = \mathbf{K} + \alpha \mathbf{I}$, where \mathbf{I} is the identity matrix and α is a positive number to ensure the positive definiteness of \mathbf{K}^* which guarantees $\mathbf{u} \cdot \mathbf{P} > 0$. It is important to note that the state of minimal energy is independent of α . This is because the energy minimum is characterized by $\mathbf{P} = \mathbf{0}$, and independent of \mathbf{K} or \mathbf{K}^* . In fact, at (and near) the state of minimum energy, such modification of \mathbf{K} is unnecessary because the stiffness matrix \mathbf{K} becomes positive definite.

We use an example of a (7,7) armchair carbon nanotube under compression to examine the stability of AFEM. Fig. 5 shows three stages of a 6 nm-long carbon nanotube at the compression strains of 0%, 6% (prior to bifurcation), and 7% (post-bifurcation). The stiffness matrix \mathbf{K} experiences non-positive definiteness between the last two stages, but becomes positive definite again near the final stage. The bifurcation pattern and the corresponding bifurcation strain (7%) agree well with Yakobson et al.'s molecular mechanics studies [27].

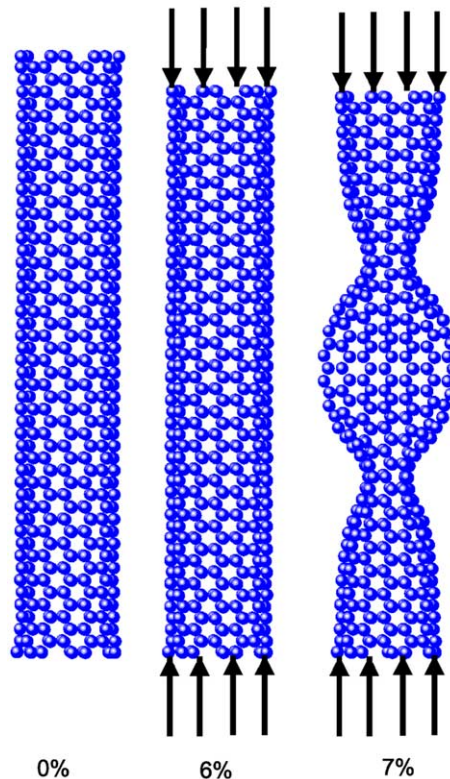


Fig. 5. Deformation patterns for a 6 nm-long (7,7) carbon nanotube under compression predicted by atomic-scale finite element method (AFEM). Bifurcation occurs at 7% compressive strain. This shows that AFEM is stable.

5. AFEM/FEM multiscale computation method

One advantage of AFEM is that it can be readily linked with the conventional continuum FEM since they are in the same theoretical framework. The AFEM/FEM linkage provides a seamless multiscale computation method for static analysis because $\mathbf{Ku} = \mathbf{P}$ in Eq. (5) gives a unified governing equation for both AFEM and FEM. In fact, we have implemented the AFEM element in the ABAQUS finite element program [1] via its USER-ELEMENT subroutine, and have studied several atomic-scale problems in this paper. We have also combined AFEM/FEM elements for multiscale computation.

In order to ensure that the AFEM/FEM multiscale computation method accurately represents the material behavior at both atomic and continuum scales, the continuum FEM elements should be based on the same interatomic potential as AFEM elements. Furthermore, similar to the use of different types of elements in conventional FEM, it is necessary to develop the transitional elements in order to smoothly link AFEM and FEM elements. These two issues are addressed in Sections 5.1 and 5.2, respectively.

5.1. The (local) continuum elements based on the (non-local) interatomic potential

The conventional continuum elements based on the phenomenological constitutive models will lead to computation errors if used in multiscale computation. There are significant efforts to develop new

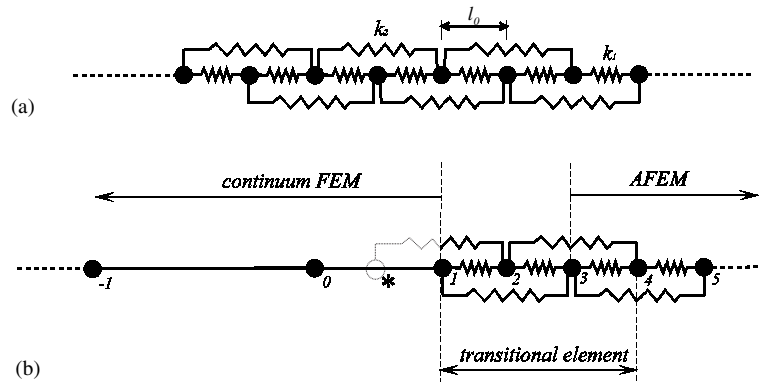


Fig. 6. (a) A schematic diagram of a one-dimensional atomic chain with local and non-local atomistic interactions characterized by the nearest-neighbor and second nearest-neighbor springs, respectively. The equilibrium distance between atoms is l_0 . The spring constants are k_1 and k_2 . (b) A schematic diagram of the transitional element between continuum and atomic-scale finite elements. The transitional element overlaps with the atomic-scale finite elements, but does not overlap with the continuum finite element.

constitutive models on the continuum level directly from the atomic structure and the interatomic potential (e.g., [2,5,11,14,15,17]). These are achieved by the Cauchy–Born rule [5] to equate the continuum strain energy to the energy in atomic bonds. These lead to local constitutive models for non-local (multi-body) interatomic potentials. By replacing the phenomenological constitutive models in the conventional FEM with the interatomic potential-based constitutive models, one obtains the new continuum elements representing the collective behavior of atoms. Zhang et al. [29–31] and Huang and Wang [13] provided details of this approach for carbon nanotubes.

We use the one-dimensional atomic chain in Fig. 6a with non-local atomistic interactions to illustrate this approach. The equilibrium distance between atoms is denoted by l_0 . Each atom is connected to its nearest-neighbor atoms by linear springs with the spring constant k_1 . To illustrate the non-local atomistic interactions, each atom is also connected to its second nearest-neighbor atoms via springs, and the spring constant is k_2 . For a given strain ε , a bond between nearest-neighbor atoms is stretched by $l_0\varepsilon$, and the energy stored in the bond is $E_1 = \frac{1}{2}k_1(l_0\varepsilon)^2$. A bond between second nearest-neighbor atoms is stretched by $2l_0\varepsilon$, and the corresponding energy in the bond is $E_2 = \frac{1}{2}k_2(2l_0\varepsilon)^2$. From the Cauchy–Born rule [5], the strain energy per unit length for this atomic chain is $(2E_1 + 2E_2)/(2l_0) = \frac{1}{2}(k_1 + 4k_2)l_0\varepsilon^2$. This gives a tensile stiffness $(k_1 + 4k_2)l_0$ in the local, continuum constitutive model for this one-dimensional atomic chain. Therefore, an atomic chain of length L with the above non-local atomistic interactions is equivalent a local spring element with a spring constant $(k_1 + 4k_2)l_0/L$.

5.2. Transitional elements between AFEM and continuum FEM elements

The transitional elements ensure the smooth transition between AFEM and continuum FEM elements. They are important to ensure the accuracy of multiscale computation linking the domains of discrete atoms and continuum solids. The transitional elements should satisfy the following requirements:

- (i) A transitional element should possess both non-local and local features in order to interface with AFEM and continuum FEM elements.
- (ii) A transitional element must survive the “patch test”, i.e., it should give accurate results for uniform deformation.

Fig. 6b shows a transitional element between a (local) continuum element (denoted by the solid line) and (non-local) AFEM elements for the one-dimensional atomic chain in Fig. 6a. The transitional element made of atoms #1, 2, 3, and 4 (Fig. 6b) overlaps with the AFEM elements but does not overlap with the continuum elements, which reflects the non-local nature of AFEM elements and the local nature of continuum elements. The nodes 1, 0, -1, -2, . . . are for continuum elements, while nodes 1, 2, 3, 4, . . . are atoms for AFEM and transitional elements. The derivatives of energy with respect to continuum nodes ($i \leq 0$) $\frac{\partial U_{\text{tot}}}{\partial x_i}$ are obtained from the standard conventional FEM. The derivatives $\frac{\partial U_{\text{tot}}}{\partial x_i}$ with respect to all atoms $i \geq 3$ (i.e., excluding the first two in the transitional element) can be obtained from the corresponding AFEM element for atom i . In the following we evaluate $\frac{\partial U_{\text{tot}}}{\partial x_1}$ and $\frac{\partial U_{\text{tot}}}{\partial x_2}$.

The energy related to atom 1 is composed of the parts from continuum element 0–1 (between nodes 0 and 1) and from the transition element, i.e.,

$$\frac{\partial U_{\text{tot}}}{\partial x_1} = \frac{\partial U_{0-1}^{\text{element}}}{\partial x_1} + \frac{\partial}{\partial x_1} \left[\frac{1}{2} k_1 (x_2 - x_1 - l_0)^2 + \frac{1}{2} k_2 (x_3 - x_1 - 2l_0)^2 \right]. \quad (12)$$

The energy related to atom 2 is given by

$$\frac{\partial U_{\text{tot}}}{\partial x_2} = \frac{\partial}{\partial x_2} \left[\frac{1}{2} k_1 (x_2 - x_1 - l_0)^2 + \frac{1}{2} k_1 (x_3 - x_2 - l_0)^2 + \frac{1}{2} k_2 (x_4 - x_2 - 2l_0)^2 + \frac{1}{2} \cdot \frac{1}{2} k_2 (x_2 - x_* - 2l_0)^2 \right], \quad (13)$$

where the extra 1/2 in front of the last term on the right hand side results from half of the energy in the spring connecting atom 2 in the transitional element to atom * in the continuum element. In order to determine x_* from the nodes in the transitional element, we approximate it by extrapolation $x_* = 2x_1 - x_2$.

For the one-dimensional atomic chain in Fig. 6a with the spring constant $k_1 = k_2 = k$, we have used the combined AFEM/FEM to calculate the displacement in the chain. The continuum elements are used near both ends of the chain, while AFEM elements are used in the central part. We have conducted the patch test with and without the transitional elements. Fig. 7 shows the displacement in the chain whose left node is fixed and right node is subject to a force $F = kl_0$. It is clearly observed that the deformation predicted by AFEM/FEM with transitional elements is uniform, which is consistent with the analytic solution for this problem. Without the transitional elements, the displacements display errors mainly around the interfaces between AFEM and continuum FEM elements. These errors are attributed to the ghost force at the interfaces. But the proper use of transitional elements can eliminate the ghost force.

The above example also provides some insights into the development of transitional elements for other systems. First, it is important to realize that, the transition elements also depend on the atomic structure of the material, similar to AFEM and continuum elements based on the interatomic potential. Secondly, the calculation of energy related to nodes in the transitional elements may require some extrapolations of atom positions (e.g., * in Fig. 6b) due to the non-local nature of atomistic interactions.

5.3. AFEM/FEM multiscale computation

In order to demonstrate the AFEM/FEM multiscale computation, we have calculated a 605 nm-long (5, 5) armchair carbon nanotube with 48,200 atoms (Fig. 8). The carbon nanotube has two fixed ends, and is subject to a displacement of 81 nm in the middle, resulting in 15° rotation at the two fixed ends as in Tomblor et al.'s experiment [25]. Two computational schemes are adopted. In the first scheme (Fig. 8a), only AFEM elements are used and there are 48,200 elements. In the second scheme (Fig. 8b), AFEM elements are used for the middle portion of the carbon nanotube having 800 carbon atoms where the deformation is highly non-uniform, while the rest of the carbon nanotube is modeled by continuum FEM elements, which are linked to AFEM elements via two transitional elements. Two FEM string elements are

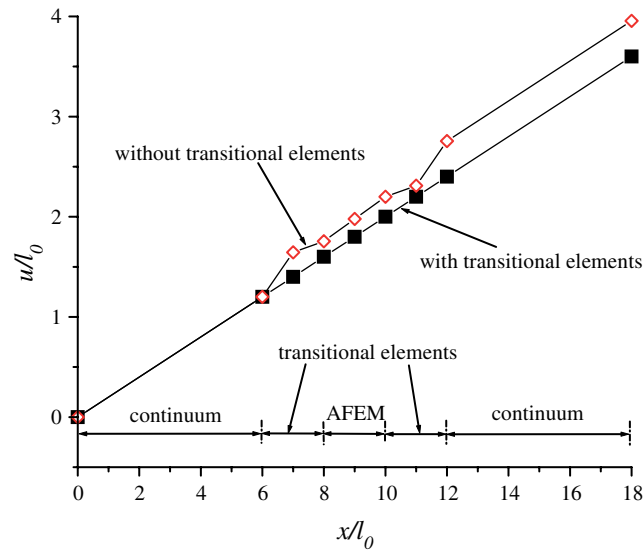


Fig. 7. The linkage between atomic-scale and continuum finite elements for a one-dimensional atomic chain. The linkage with the transitional elements shows accurate displacements, while that without the transitional elements clearly shows errors.

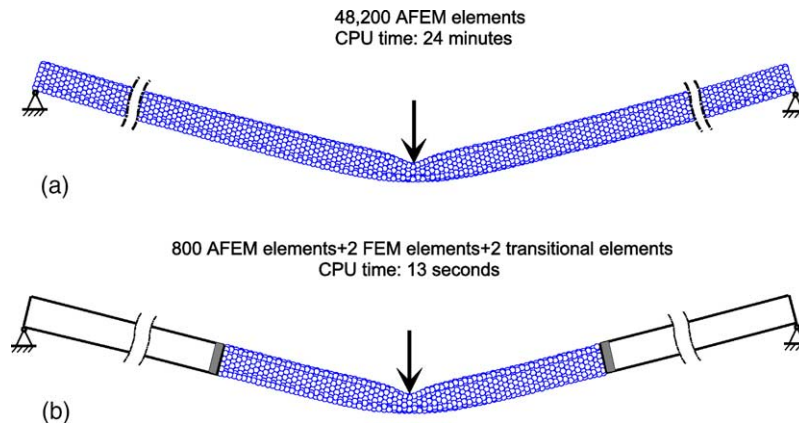


Fig. 8. A 605 nm-long (5,5) carbon nanotube with 48,200 atoms subject to 81 nm deflection in the middle. AFEM takes 24 min to determine atom positions, while combined AFEM/FEM takes only 13 s. This shows that combined AFEM/FEM is an efficient multiscale computational method.

used and their tensile stiffness determined from the interatomic potential of carbon [31]. The differences between the results obtained from two schemes are less than 1%. However, the CPU time in the second scheme is only 13 s (on a personal computer with 2.8 GHz CPU and 1 GB memory), which is less than 1% of that in the first scheme, 24 min. Moreover, the saving in computer memory is also tremendous since the second scheme requires less than 2% memory of the first one.

6. Applications of AFEM

6.1. Multiple atomistic interactions

AFEM can be combined with other elements to simultaneously account for multiple interactions among atoms, such as the covalent bond and van der Waals interactions. These two atomistic interactions govern the equilibrium state of a (5, 5) armchair carbon nanotube knot. The van der Waals interactions between carbon atoms from the contacting parts of the carbon nanotube are critical to the knot formation and evolution under load, and therefore must be accounted for. The van der Waals interactions for carbon [12] are included via nonlinear string elements, and they are accounted for only when the distance between two carbon atoms is less than the cutoff radius.

Fig. 9a shows an equilibrium state of carbon nanotube knot with 10,000 atoms. The two ends of the carbon nanotube are free. The diameter of the knot at this relaxed state is approximately 23 nm. Fig. 9b shows the same carbon nanotube knot subject to horizontal displacements ± 20 nm at the two ends of the carbon nanotube, and it corresponds to the new equilibrium state for the given end displacements. The diameter of the carbon nanotube becomes much smaller, approximately 13 nm. Once the ends are released, the carbon nanotube knot in Fig. 9a is resumed. It is important to note that during this process the nonlinear string elements (for van der Waals interactions) evolve due to the significant change of distance between carbon atoms. Some existing nonlinear string elements disappear once the cutoff radius is exceeded, while some new string elements emerge once atom distance becomes smaller than the cutoff radius. This example shows that AFEM can be used to study the quasi-static evolution of nanoscale materials and systems.

6.2. Vibration frequencies and modes of carbon nanotubes

The vibration frequencies and modes of carbon nanotubes are important to various potential applications of carbon nanotubes and to their mechanical property measurement (e.g., see the review paper of Huang and Wang [13] and the references therein). It is difficult for atomistic simulation methods (e.g., molecular dynamics) to determine the frequencies and modes of a carbon nanotube. AFEM provides a straightforward way to achieve this goal since the vibration frequencies and modes can be readily obtained

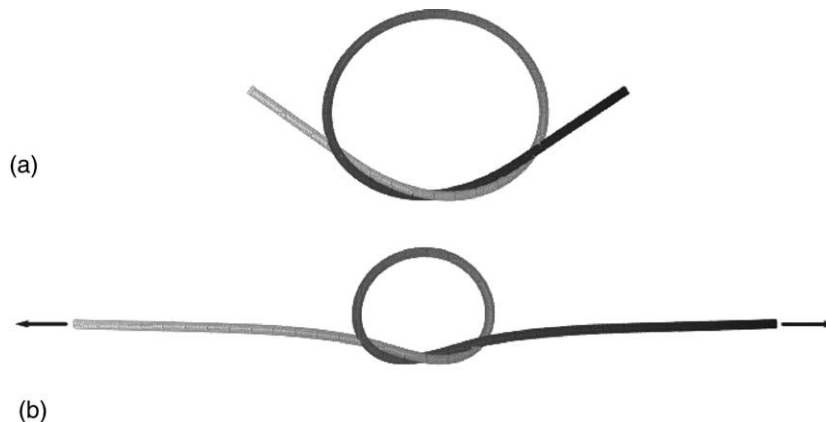


Fig. 9. A knot of (5, 5) armchair carbon nanotube with 10,000 atoms: (a) the equilibrium state, (b) the new equilibrium state subject to the end displacements ± 20 nm at the ends.

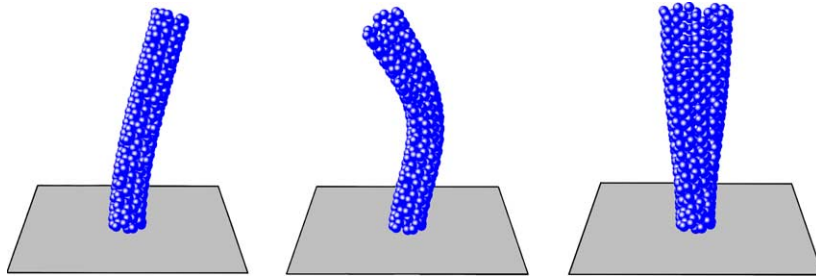


Fig. 10. The first three vibration modes of a (5,5) armchair carbon nanotube with 400 atoms and one end clamped.

from the global stiffness matrix \mathbf{K} and the mass matrix $m\mathbf{I}$, where m is the mass of a carbon atom and \mathbf{I} is the identity matrix.

We have studied the vibration of a (5,5) armchair carbon nanotube with 400 atoms. One end of the carbon nanotube is clamped. Fig. 10 shows the first three vibration modes. The corresponding frequencies are 112, 614, and 685 GHz, respectively. The first two modes are rather similar to the base modes of a cantilever beam, but the third one is very different and it corresponds to the radical expansion of the carbon nanotube (with one end fixed). This vibration mode, not captured by the existing beam models for carbon nanotubes (e.g., see the review paper of Huang and Wang [13]), can be easily studied by AFEM.

7. Discussion and concluding remarks

We have developed an AFEM that extends the finite element method (FEM) down to the atomic scale. It does not involve any approximations of conventional FEM (e.g., shape functions), and is as accurate as molecular mechanics simulations. It is an order- N method such that the computation scales linearly with the system size N . It is therefore much faster than the widely used order- N^2 conjugate gradient method, and is suitable for large scale computations. The combination of AFEM and continuum FEM provides a seamless multiscale computation method, and is suitable for even larger scale static problems. The method can also account for multiple atomistic interactions (e.g., van der Waals interaction), as well as the evolution of atomic structures.

AFEM is also applicable to many atomistic studies since it can incorporate other atomistic models such as tight-binding potential. Together with parallel computation technique, the combined AFEM/FEM is most effective for treating problems with a large number of degrees of freedom to take advantage of its order- N nature, and therefore significantly increases the speed and limit in large scale computation. Many optimization problems involving a large number of variables can also be efficiently solved with this order- N method if the corresponding \mathbf{K} (second order derivative matrix) is sparse.

Acknowledgements

This research was supported by NSF (grants 00-99909 and 01-03257), ASCI Center for Simulation of Advanced Rockets at the University of Illinois supported by US Department of Energy through the University of California under subcontract B523819, and NSFC.

References

- [1] ABAQUS, ABAQUS Theory Manual and Users Manual, version 6.2, Hibbit, Karlsson and Sorensen Inc., Pawtucket, RI, USA, 2002.
- [2] M. Arroyo, T. Belytschko, An atomistic-based finite deformation membrane for single layer crystalline films, *J. Mech. Phys. Solids* 50 (9) (2002) 1941–1977.
- [3] F.F. Abraham, R. Walkup, H.J. Gao, M. Duchaineau, T.D. De la Rubia, M. Seager, Simulating materials failure by using up to one billion atoms and the world's fastest computer: brittle fracture, in: *Proceedings of the National Academy of Sciences of the United States of America*, vol. 99, no. 9, 2002, pp. 5777–5782.
- [4] F.F. Abraham, R. Walkup, H.J. Gao, M. Duchaineau, T.D. De la Rubia, M. Seager, Simulating materials failure by using up to one billion atoms and the world's fastest computer: work-hardening, in: *Proceedings of the National Academy of Sciences of the United States of America*, vol. 99, no. 9, 2002, pp. 5783–5787.
- [5] M. Born, K. Huang, *Dynamical Theory of the Crystal Lattices*, Oxford University Press, Oxford, 1954.
- [6] D.W. Brenner, Empirical potential for hydrocarbons for use in simulating the chemical vapor deposition of diamond films, *Phys. Rev. B* 42 (1990) 9458–9471.
- [7] D.W. Brenner, O.A. Shenderova, J.A. Harrison, S.J. Stuart, B. Ni, S.B. Sinnott, A second-generation reactive empirical bond order (REBO) potential energy expression for hydrocarbons, *J. Phys.: Condens. Matter* 14 (4) (2002) 783–802.
- [8] W.A. Curtin, R.E. Miller, Atomistic/continuum coupling in computational materials science, *Model. Simulat. Mater. Sci. Eng.* 11 (3) (2003) R33–R68.
- [9] S. Curtarolo, G. Ceder, Dynamics of an inhomogeneously coarse grained multiscale system, *Phys. Rev. Lett.* 88 (2002) 255504.
- [10] W. E, Z. Huang, Matching conditions in atomistic–continuum modeling of materials, *Phys. Rev. Lett.* 87 (2001) 135501.
- [11] H.J. Gao, P. Klein, Numerical simulation of crack growth in an isotropic solid with randomized internal cohesive bonds, *J. Mech. Phys. Solids* 46 (1998) 187–218.
- [12] L.A. Girifalco, M. Hodak, R.S. Lee, Carbon nanotubes, buckyballs, ropes, and a universal graphitic potential, *Phys. Rev. B* 62 (19) (2000) 13104–13110.
- [13] Y. Huang, Z.L. Wang, Mechanics of carbon nanotubes, in: B. Karihaloo, R. Ritchie, I. Milne (Eds.), *Interfacial and Nanoscale Fracture*, in: W. Gerberich, W. Yang (Eds.), *Comprehensive Structural Integrity Handbook*, vol. 8, 2003, pp. 551–579 (Chapter 8.16).
- [14] P. Klein, H. Gao, Crack nucleation and growth as strain localization in a virtual-bond continuum, *Engrg. Fract. Mech.* 61 (1998) 21–48.
- [15] P. Klein, H. Gao, Study of crack dynamics using the virtual internal bond method, in: *Multiscale deformation and fracture in materials and structures*, James R. Rice's 60th Anniversary Volume, Kluwer Academic Publishers, Dordrecht, The Netherlands, 2000, pp. 275–309.
- [16] S. Kohlhoff, P. Gumbsch, H.F. Fischmeister, Crack-propagation in bcc crystals studied with a combined finite-element and atomistic model, *Philos. Mag. A* 64 (1991) 851–878.
- [17] F. Milstein, Review: theoretical elastic behaviour at large strains, *J. Mater. Sci.* 15 (1980) 1071–1084.
- [18] G.E. Moore, Cramming more components onto integrated circuits, *Electronics* 38 (8) (1965).
- [19] W.H. Press, B.P. Flannery, S.A. Teukolsky, W.T. Vetterling, *Numerical Recipes*, Cambridge University Press, New York, 1986.
- [20] H. Rafii-Tabar, L. Hua, M. Cross, A multi-scale atomistic–continuum modelling of crack propagation in a two-dimensional macroscopic plate, *J. Phys.: Condens. Matter* 10 (1998) 2375–2387.
- [21] R.E. Rudd, J.Q. Broughton, Concurrent coupling of length scales in solid state systems, *Phys. Stat. Sol. B—Basic Res.* 217 (1) (2000) 251–291.
- [22] V.B. Shenoy, R. Miller, E.B. Tadmor, D. Rodney, R. Phillips, M. Ortiz, An adaptive finite element approach to atomic-scale mechanics—the quasicontinuum method, *J. Mech. Phys. Solids* 47 (3) (1999) 611–642.
- [23] L.E. Shilkrot, W.A. Curtin, R.E. Miller, A coupled atomistic/continuum model of defects in solids, *J. Mech. Phys. Solids* 50 (10) (2002) 2085–2106.
- [24] E.B. Tadmor, M. Ortiz, R. Phillips, Quasicontinuum analysis of defects in solids, *Philos. Mag. A—Phys. Condens. Matter Struct. Def. Mech. Properties* 73 (6) (1996) 1529–1563.
- [25] T.W. Tomblor, C. Zhou, L. Alexseyev, J. Kong, H. Dai, L. Liu, C.S. Jayanthi, M. Tang, S.-Y. Wu, Reversible electromechanical characteristics of carbon nanotubes under local probe manipulation, *Nature* 405 (2000) 769–772.
- [26] G.J. Wagner, W.K. Liu, Coupling of atomistic and continuum simulations using bridging scale decomposition, *J. Comput. Phys.* 190 (2003) 249–274.
- [27] B.I. Yakobson, C.J. Brabec, J. Bernholc, Nanomechanics of carbon tubes: instabilities beyond linear response, *Phys. Rev. Lett.* 76 (1996) 2511–2514.
- [28] W. Yang, H. Tan, T.F. Guo, Evolution of crack-tip process zones, *Model. Simulat. Mater. Sci. Eng.* 2 (1994) 767–782.
- [29] P. Zhang, H. Jiang, Y. Huang, P.H. Geubelle, K.C. Hwang, An atomistic-based continuum theory for carbon nanotubes: analysis of fracture nucleation, *J. Mech. Phys. Solids*, in press.

- [30] P. Zhang, Y. Huang, P.H. Geubelle, K.C. Hwang, On the continuum modeling of carbon nanotubes, *Acta Mech. Sinica* 18 (2002) 528–536.
- [31] P. Zhang, Y. Huang, P.H. Geubelle, P.A. Klein, K.C. Hwang, The elastic modulus of single-wall carbon nanotubes: a continuum analysis incorporating interatomic potentials, *Int. J. Sol. Struct.* 39 (2002) 3893–3906.